Computers and Geotechnics 166 (2024) 105991

Contents lists available at ScienceDirect

Computers and Geotechnics

journal homepage: www.elsevier.com/locate/compgeo

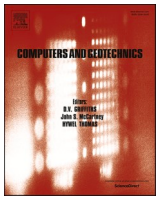

Effects of pre-shearing stress ratio on the mechanical behaviours of gap-graded soils subjected to internal erosion

Tien V. Nguyen [a], Ha H. Bui [a,*], Khoa M. Tran [a], Giang D. Nguyen [b], Asadul Haque [a]

[a] Department of Civil Engineering, Monash University, Australia
[b] School of Architecture and Civil Engineering, The University of Adelaide, Australia

ARTICLE INFO

Keywords:
DEM
Internal erosion
Suffusion
Suffosion
Gap-graded soils
Pre-shearing stress

ABSTRACT

Internal erosion can induce significant changes in the mechanical properties of soils, posing various hazards to dam and dike structures. Despite its importance, our current understanding of this phenomenon remains incomplete. The influence of pre-shearing stress conditions on the mechanical behaviours of soils during the internal erosion process is particularly challenging, as existing experiments have not been able to maintain the constant pre-shearing stress ratios. To bridge this gap in knowledge, this paper presents a series of discrete element method (DEM) simulations focused on gap-graded cohesionless soil. The primary objective of these simulations is to investigate two specific cases of internal erosion: suffusion and suffosion processes. Soil specimens are subjected to different pre-shearing stress ratios in the standard triaxial tests before being submitted to different levels of erosion to study their constitutive responses. The results show that erosion-induced deformation (i.e. suffosion) only starts after a specific amount of mass loss. This mass loss and the pre-shearing stress ratio form a well-defined criterion for triggering suffosion, which is named "*suffosion surface*". The volumetric strain is shown to be a better indicator to describe the suffosion process than the commonly used void ratio. The pre-shearing stress ratio significantly influences the suffosion response of the soil sample, with a higher pre-shearing stress ratio facilitating soil failure. Furthermore, soil specimens undergo both deviatoric and volumetric responses during the suffosion process. To this end, new DEM-based statistical equations were proposed to describe the observed mechanisms, which are helpful for the future development of constitutive models to describe internal soil erosion.

1. Introduction

Internal erosion is the process in which fine soil particles are migrated in porous media under the effect of seepage flow. The occurrence of internal erosion causes porous media to lose soil grains, inducing significant changes in soils properties (e.g., an increase in the porosity, compressibility of soil, a reduction in shear strength), which, in turn, may cause many catastrophic events such as dam/embankment failures, landslides and sinkholes (Reclamation, B.o. Teton Dam History., 2016; Sawicki and Swidzinski, 2000; Mitchell and Fitzpatrick, 1979; Fisher et al., 2016; Jiang, 2023; Ye and Liu, 2021). To understand key mechanisms and effects of internal erosion on soil behaviour and to formulate criteria to assess the susceptibility of soils subjected to internal erosion, as well as to forming erosion laws, a large number of experimental studies were conducted using typical tests such as hydraulic tests (Israr et al., 2016; Chang and Zhang, 2013; Lafleur et al., 1989), triaxial tests integrated with pressurised water supply system (Chang and Zhang, 2011; Chang and Zhang, 2013; Ke and Takahashi, 2014). Although these studies have provided valuable empirical criteria (Chang and Zhang, 2013; Sherard, 1992. 1992.; Kenney and Lau, 1985; Wan and Fell, 2008; Fannin, 2008) for assessing the susceptibility of soils and hydraulic conditions due to internal erosion, and revealed typical post-eroded responses of soils (e.g., increase in hydraulic conductivity and compressibility, decreases in shear strength), insights into the underlying mechanisms governing internal soil erosion are still far from comprehensive. Contradicting results have been reported in the literature. For example, there exists a disagreement on whether soil samples become stronger or weaker (Chang and Zhang, 2011; Ke et al., 2012; Xiao and Shwiyhat, 2012; Ke and Takahashi, 2014) after internal soil erosion. This is because the mechanical behaviours of sandy soils are affected by multiple internal/external factors, including particle sizes, shapes (Zhou, 2016; Dai et al., 2016; Wei and Yang, 2014; Slangen and

* Corresponding author at: Department of Civil Engineering, Monash University, Australia.
E-mail address: ha.bui@monash.edu (H.H. Bui).

https://doi.org/10.1016/j.compgeo.2023.105991
Received 28 July 2023; Received in revised form 29 November 2023; Accepted 29 November 2023
Available online 10 December 2023

Fannin, 2017; Cavarretta et al., 2010), grain size distributions (GSDs) (Xiao, 2017; Strahler et al., 2018; Prasomsri et al., 2021), confining pressures (Xiao, 2017) and stress paths (Xu et al., 2012). In addition, internal erosion results in complicated interactions between many different processes, including narrower GSD (Zhang, 2019), increases in hydraulic conductivity (Hieu et al., 2017), changes in the pore network (Nguyen, 2019), and soil stress states (Ke and Takahashi, 2012; Scholtes et al., 2010; Wood et al., 2010). Moreover, most existing experimental studies have overlooked the effect of pre-shearing stress ratios on the mechanical behaviours of soils during the internal erosion process, as it has been challenging to maintain constant pre-shearing stress ratios using existing experimental apparatuses. This limitation raises concerns about the applicability of existing experimental findings to real in-situ conditions.

To address the above difficulties, the discrete element method (DEM) (Cundall and Strack, 1979) has been utilised and shown to be a promising tool to improve our understanding of internal soil erosion (Scholtes et al., 2010; Wood et al., 2010; Wang and Li, 2015; Shire, 2014; Nguyen and Indraratna, 2020). Shire, O'Sullivan (Shire, 2014) reported that lower effective stress transmitting through finer particles is the main reason causing fine particles to be eroded. The effective stress distribution inside the soil specimen significantly depends on its particle-size distribution, particle shape, finer fraction percentage and relative density. Changes in the dilatancy response (i.e. from dilatant to contractive behaviours) and stress states of the soil specimen caused by internal erosion were also highlighted in several previous studies by Muir Wood, Maeda (Wood et al., 2010)and Scholtes, Hicher and Sibille (Scholtes et al., 2010). In addition, DEM has also been coupled with computational fluid dynamics (CFD) to replicate seepage flow and subsequent internal erosion. For example, Tao and Tao (Tao and Tao, 2017) reported that the evolution of piping depends heavily on the particle size and porosity distribution and that piping does not always initiate from the free surface. Zheng et al (Hu et al., 2019) investigated the progressive loss of fine particles subjected to upward seepage flow on suffusion in gap-graded and well-graded soils and indicated that the loss of the cumulative fine approaches the initial fines content at the end of suffusion for the gap-graded soils, while is negligible for well-graded soils. Overall, existing DEM studies have provided a better understanding of changes in soil fabrics and some important soil responses caused by internal erosion. However, very limited research (if not any) was dedicated to studying the suffosion process (i.e. how the soil deforms during internal erosion) and to investigating its consequence on the overall behaviour of soil samples when being further subjected to different pre-shearing conditions.

In this study, the effect of internal soil erosion on suffusion and suffosion responses of gap-graded soil is quantitatively investigated using 3D DEM simulations. Different amounts of erosion, confining stresses and pre-shearing stress ratios are applied in these simulations to achieve insights into the understanding of the mechanical responses of gap-graded soils at different states during the internal erosion process. New DEM-based statistical equations are then proposed to describe key mechanisms underpinning the internal erosion processes.

2. Numerical procedures

Standard triaxial tests were numerically carried out on gap-graded soil samples to investigate the behaviour of these samples under different loading processes. The soil sample has a cubic shape with a dimension of ($10 \times 10 \times 10$ mm) and an initial fines content of 35 %. All the DEM simulations are implemented in the YADE software package (Kozicki and Donze, 2009). Soil samples were created using the radius expansion method, commonly used in the literature (Lee et al., 2012; Tran et al., 2021; Tran, 2020; Mu, 2023), and each soil sample has approximately 150,000 spherical particles. The GSD was selected so that the generated samples were internally unstable and vulnerable to seepage flow (KÉZDI, Á., Soil Physics: Selected Topics., 1979; Kenney and Lau, 1986; Kenney and Lau, 1985; Burenkova, 1993). A similar configuration was also previously considered by Shire, O'Sullivan (Shire, 2014) and Kenichi Kawano (Kawano, 2016). Confining pressure was applied to the samples by applying the servo-control to the six frictionless walls. Fig. 1 shows the GSD of a soil sample with an initial fines content of 35 % and a numerical sample after being confined at 100 kPa. Fig. 2 shows the triaxial loading paths of non-eroded samples at different confining stresses and the estimated critical state line (CSL) for these samples generated using the initial interpaticle friction of 0.1. It can be observed from this figure that the initial states of these samples are located well below the CSL, indicating relatively dense samples. On the other hand, for samples generated using the initial interpaticle friction of 0.2, their initial void ratio is around 0.36 for a confining pressure ranging from 50 kPa − 200 kPa. This range of initial void ratio falls just above the CSL, suggesting that these samples are in the medium-dense state. Other basic parameters for DEM simulations in this study are summarised in Table 1.

The erosion and shearing processes are outlined in Fig. 3*(a)*. After being isotropically confined and reaching their equilibrium state, soil specimens were moved into the pre-shearing stage to reproduce field conditions where different pre-shearing stress ratios were applied to the soil body. The macroscopic response of the samples during the pre-shearing state is indicated by line segments AB and AB′ in Fig. 3 *(b)*. After a desired pre-shearing stress ratio $\eta = q/p$ (with q being the deviatoric stress and p the mean stress) was achieved, the soil specimen was then subjected to the erosion process represented by line segments BC and B′C′ in Fig. 3 *(b)*. This process was accomplished by following the approach reported by Scholtes, Hicher and Sibille (Scholtes et al., 2010), in which particles that carried the smallest stress were slowly shrunk and subsequently removed from the soil specimen after their size was less than 10 % of the initial size of the smallest particle. Each time particles were shrunk or deleted, the samples were run until reaching their equilibrium state, and then the above steps were repeated until the specified eroded fraction (i.e., the ratio of the eroded mass to the initial mass) was achieved. The stress ratio and confining stress were kept constant during this erosion process. Fig. 1 shows the GSD evolution of a sample after being eroded from 0 % to 12.5 % fines content at different specified eroded fractions, which is consistent with previous studies (Scholtes et al., 2010; Wood et al., 2010; Hicher, 2013; Hosn, 2018; Wang and Li, 2015). To distinguish samples tested in this study, the samples, hereafter, are named corresponding to the stages they experienced. For example, p100d5 refers to a dense (d) sample with an initial confining pressure (p) of 100 kPa and undergoing 5 % erosion (e). It is worth noting that all samples used in this paper are dense. Samples generated with an initial inter-particle friction of 0.1 (denoted with the letter d in the sample name) are denser than those created using an initial inter-particle friction of 0.2 (without the letter d).

3. Influence of internal erosion on pre-shared samples

3.1. The onset of deformation – Suffosion surface

Gap-graded soils consist of fine particles filled up void spaces created by coarse particles, and thus under external loads, soil particles of different sizes could bear different levels of stress. When these soils are subjected to internal erosion with a large enough hydraulic gradient, stress-free fine particles (or very lightly stressed) may be eroded first. The mass loss of these fine particles, in many cases, does not trigger any soil deformation or affect the stability of the soil samples in the short term. This process is often named "suffusion". As more fine particles are eroded, the soil samples start to deform, causing instability to the soil samples, and this process is commonly named "suffosion". The transition limit between suffusion and suffosion or the onset of deformation is hereafter termed the "suffosion point". Shire, O'Sullivan (Shire, 2014) reported that the suffosion point of gap-graded soils changes with the gap ratios and fines fractions. In our view, stress states may also affect

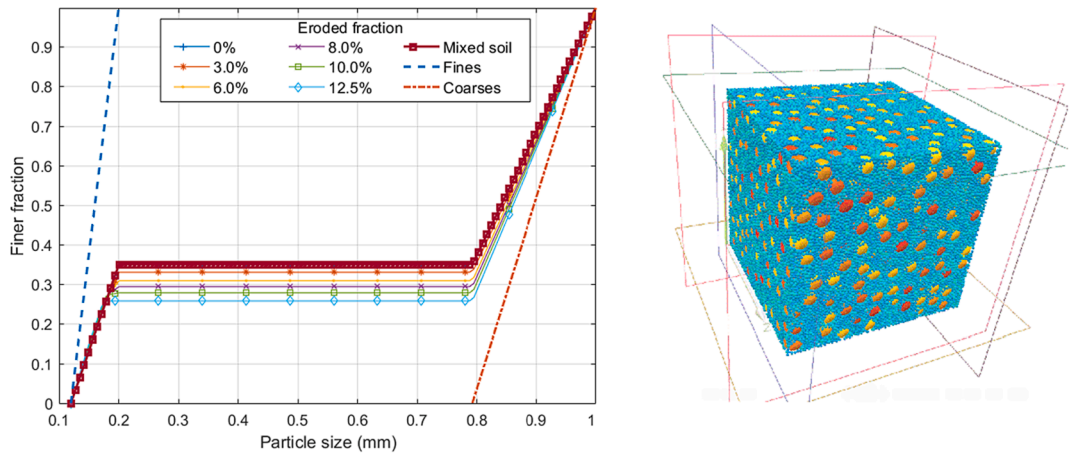

Fig. 1. GSD of DEM sample at different levels of erosion.

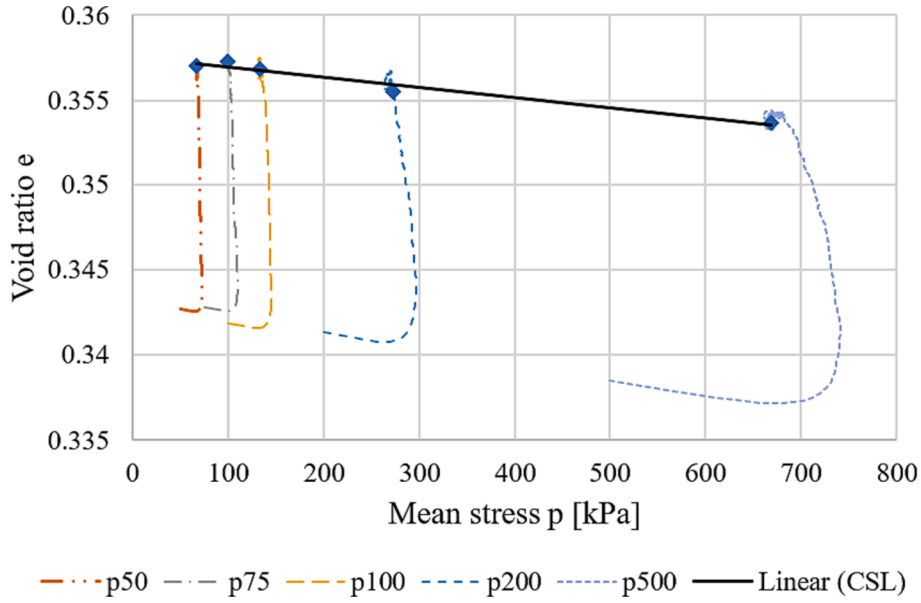

Fig. 2. Triaxial loading paths and an approximated critical state line for non-eroded samples at different confining stresses ($\mu_i = 0.1$).

Table 1
Input parameter for DEM simulations.

Parameter	Symbol	Value		Unit
Particle density	ρ	2670		kg/m^3
Initial inter-particle friction*	μ i	0.1	0.2	
Initial void ratio (after confining)	e	0.339–0.342	0.359–0.360	
Final inter-particle friction	μ f	0.3		
Particle Young's modulus	E	5.00×10^8		Pa
Poisson's ratio	υ	0.3		
Confining stress	p	50 to 700		kPa
Erosion percentage	f_{er}	0 to 12.5		%
Maximum wall Velocity	v_{wall_max}	0.05 to 1		m/s

* The initial inter-particle friction of 0.1 is used to create dense samples (denoted with the letter d in the sample name), while that of 0.2 is used for other samples.

this suffosion point as under a higher stress state, more particles are involved in carrying external loads, and thus the sample is more likely to deform given the same amount of erosion.

To quantitatively determine the suffosion point under different stress states, the evolution of volumetric strain caused by internal erosion was recorded during the first stage of eroding soil samples. It is important to note that in DEM simulations, the measurement of sample deformation due to particle removal is instantaneous. In contrast, achieving this in the laboratory with exisiting equipment is not a straightforward task. To ensure the correct determination of the suffosion point in the experiment, it is crucial to consider the delay in measurement between erosion and sample deformation. Fig. 4*(a)* plots this evolution for four samples under the same confining pressure of 100 kPa and the initial state parameter, which is defined as the difference between current void ratio and critical state void ratio (the void ratio on the critical state line under the same confining stress as the current void ratio), but were subjected to different pre-shearing stress ratios. Here, the samples with and without the suffix "d" attached at the end of their name have the same critical state parameters. In all cases, the volumetric strain starts to develop as soon as the erosion process commences, making it challenging to identify the suffosion point. In fact, this is also the issue of existing literature where there is no universal approach to defining this suffosion point from both experimental and numerical data (Ke and Takahashi, 2014). We also note that the sudden jump in the volumetric deformation curve observed in our numerical simulations at large pre-shearing stress ratios was caused by the local pore collapse, which significantly varies among soil samples and thus is not suitable to

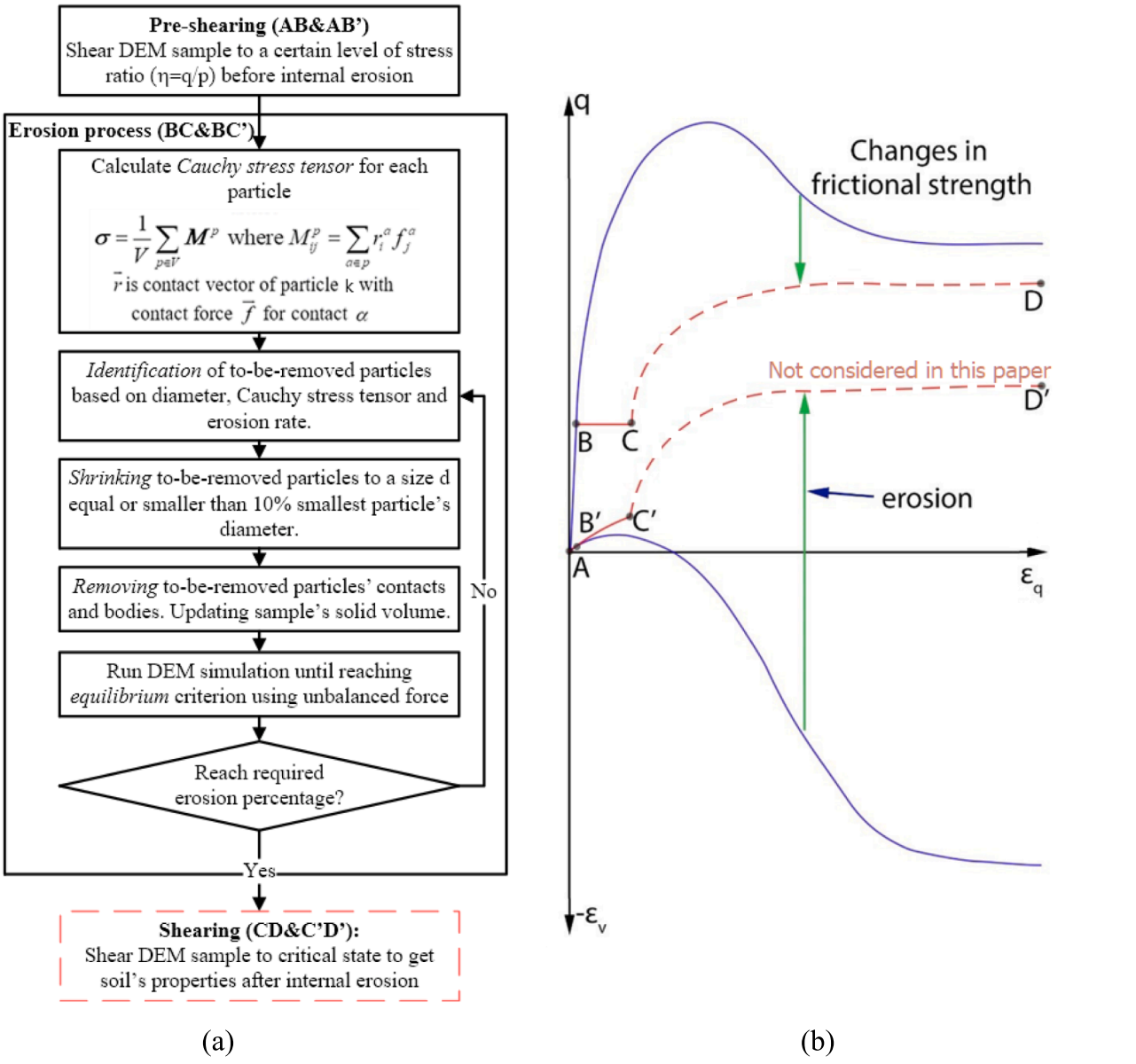

Fig. 3. Internal erosion simulation procedure: a) Internal erosion and shearing processes in DEM simulations; b) Typical volumetric and shear behaviours of a soil specimen without (blue line) and with internal erosion (red line).

represent the suffosion point. A regression approach is adopted in this work to provide a more consistent definition of the suffosion points for a range of erosion tests at different pre-shearing stress ratios. For each DEM result, a corresponding regression line is generated, as shown by the dashed lines in Fig. 4 *(a)*. The intersection between this regression line and the horizontal axis is then considered as the suffosion point. Suffosion points identified by the regression approach are marked with red dots in Fig. 4 *(a)*. The position of suffosion points of all samples subjected to different pre-shearing stress ratios is summarised in Fig. 4 *(b)*. As can be seen from this figure, the pre-shearing stress ratio significantly alters the location of the suffosion point or the eroded fraction at the transition between suffusion and suffosion. The higher the pre-shearing stress ratio, the less eroded fraction required to initiate deformation. When the pre-shearing stress ratio is greater than approximately 0.71, a small erosion would immediately trigger volumetric deformation (the eroded fraction threshold for suffosion at this time is close to 0.001 %). Our numerical tests suggest that the second-order polynomial regression provides a best-fit approximation of the DEM results with the least-square regression above 99 %. Fig. 4*b* also indicates that the confining pressure does not clearly influence the suffosion point, though some variations could still be observed. This can be attributed to the way soil samples were created in our numerical simulations. Here, all soil samples were generated in such a way that they shared the same initial state parameter regardless of their initial confining stress conditions. As a result, the initial density state and the number of free particles in the soil samples are also similar, alleviating the role of confining stress on the suffosion point. Nevertheless, a complete description of the suffosion point for a specific soil sample would require considering multiple factors, including GSD, fines content, confining stress, void ratio, critical void ratio, particle shape, and mobilised stress state. These considerations are beyond the topic of this paper. Within the scope of this paper, the suffosion surface is defined for relatively dense soils, considering a wide range of samples with different initial states (e.g., confining pressure and initial inter-particle friction).

The DEM numerical data presented in Fig. 4 *(b)* enables the definition of a "suffosion surface", which is the relationship between the eroded fraction and pre-shearing stress ratio at the suffosion point. This surface can be described by the following equation:

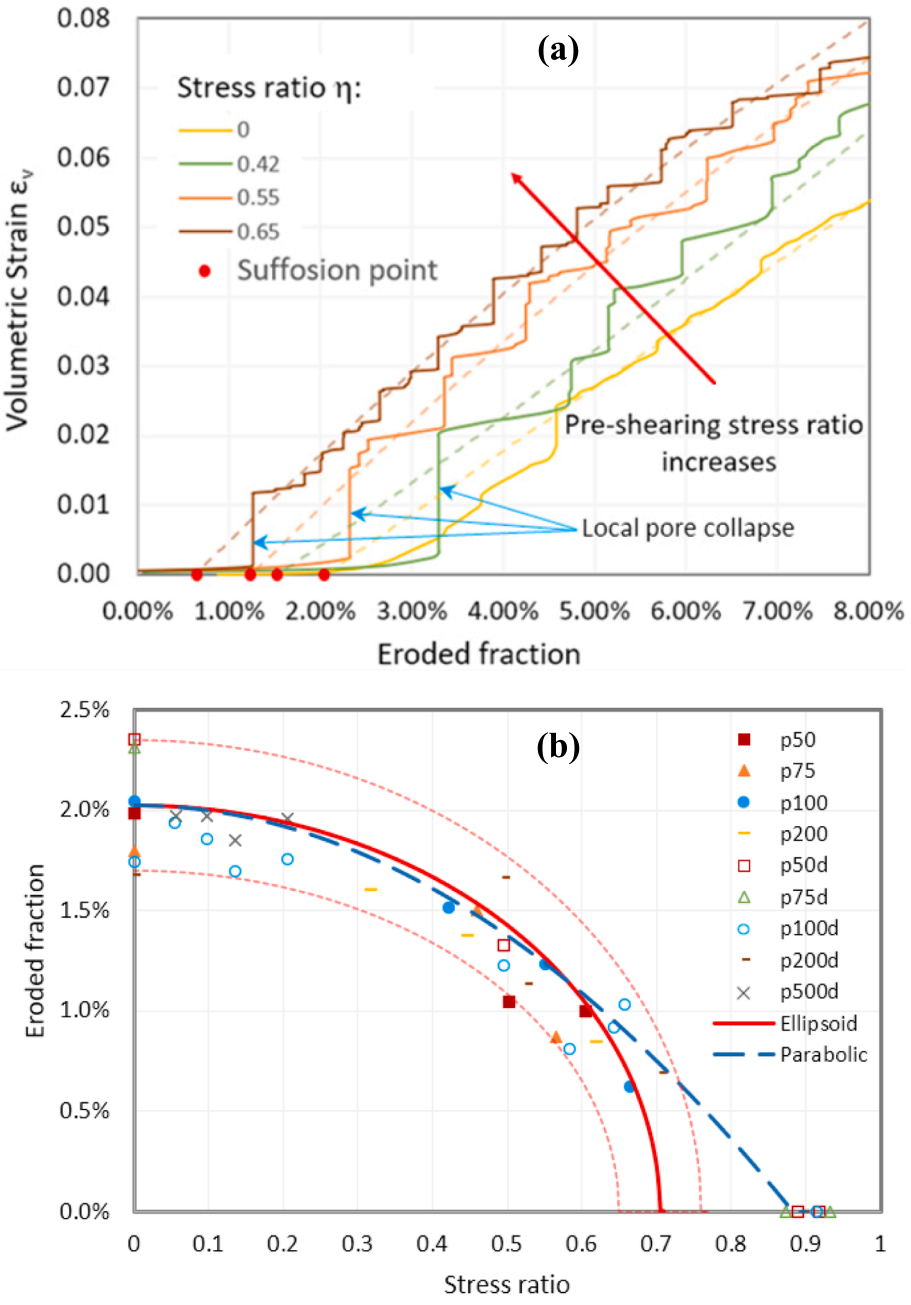

Fig. 4. Changes of suffosion points: a) Volumetric strain of samples under initial confining stress of 100 kPa and initial state parameter of −0.02; b) Suffosion point at different stress ratios.

$$\begin{cases} \left(\frac{f_{so}}{f_{so}^{\eta=0}}\right)^2 + \left(\frac{\eta}{M_c}\right)^2 = 1 & if \eta \le \eta_{\lim}^{f_{so}} \\ f_{so} = 0 & if \eta > \eta_{\lim}^{f_{so}} \end{cases} \quad (1)$$

where M_c is the slope of the critical state line in the (p, q) shear stress plane; f_{so} is the eroded fraction at which suffosion occurs; $f_{so}^{\eta=0}$ is the eroded fraction at which suffosion occurs for non-preshearing soil samples. *Equation (1)* is illustrated in Fig. 4 *(b)* by the red line with $M_c = 0.71$ and $f_{so}^{\eta=0} = 0.02$ and fits well to the numerical data generated by DEM simulations in this study. Simpler forms of mathematical expressions for the suffosion surface can also be used, for example, dual linear lines or parabolic lines, providing that those lines can best fit the experiments or numerical results. *Equation (1)* represents a significant finding for the constitutive modelling of eroded soils because it provides a criterion for deciding when the deformation (i.e., suffosion) would occur in the constitutive description of eroded soils. This equation can be fully determined from the standard erosion tests by measuring $f_{so}^{\eta=0}$, which is feasible as demonstrated in the prior work of Ke and Takahashi (Ke and Takahashi, 2014). The incorporation of this finding for constitutive modelling of eroded soils is beyond the scope of this work and will be presented in our future work.

3.2. Volumetric behaviour of granular soils due to internal erosion

Traditionally, the volumetric behaviour of soil samples subjected to internal erosion is often characterised by the volumetric strain, which is calculated based on changes in the void ratio and the amount of eroded mass (Scholtes et al., 2010; Wood et al., 2010; Hicher, 2013). The use of void ratio has advantages in generating constitutive formulas because it

is readily incorporated in the current critical state soil constitutive framework that makes use of void ratio or specific volume. However, it also poses several challenges in describing the influence of internal erosion on the volumetric behaviour of soils. This is because internal erosion causes changes to both volumetric deformation and void ratio, both of which are linked to mass loss and soil compaction or particle rearrangements. In many cases, internal erosion does not induce any change to the volumetric deformation (i.e., suffusion), but still causes changes to the void ratio. In such cases, it is invalid to establish a single equation that links the change of void ratio to internal erosion, and subsequently to make use of this equation to predict the volumetric deformation of eroded soil samples. Therefore, it would be useful to establish an alternative way to directly link internal erosion to soil deformation.

Fig. 5 describes the changes in both void ratio (blue dashed line) and volumetric strain (continuous orange line) with respect to the evolution of internal erosion under the constant external stress condition. For the non-presheared sample ($\eta = 0$), the void ratio increases linearly with an increase in the eroded fraction up to approximately 4 % and then lightly decreases and increases again. Similarly, the void ratio increases linearly with an increase in the eroded fraction up to approximately 2 % for the presheared sample ($\eta = 0.55$). Thereafter, the void ratio significantly fluctuates until the internal erosion process completes. The DEM prediction of void ratio reveals that there is less possibility of establishing a general law to characterise the evolution of void ratio for a wide range of eroded fractions and pre-shearing stress ratios. Nevertheless, most previous studies usually capped the amount of erosion at around 5 % (Scholtes et al., 2010; Wood et al., 2010; Hicher, 2013; Hosn, 2018; Wang and Li, 2015). Within this erosion range, there was a good indication that the change in void ratio can be approximated using a linear function of eroded fraction, as shown in Fig. 5 for the non-presheared sample ($\eta = 0$). This consistent result for a small range of erosion might be attributed to why the void ratio was chosen as the primary parameter to describe the deformation of soil during internal erosion.

In contrast, after the suffosion point at approximately 2 % eroded fraction for non-presheared samples, as shown in Fig. 4*(a)* and Fig. 5*(a)*, the volumetric strain increases almost linearly with an increase in the eroded fraction. This result suggests that it would be more beneficial to use the volumetric strain as a direct link to account for the influence of internal erosion on the volumetric behaviour of eroded soil samples. This can be achieved by establishing a unique relationship between the rate of change of internal erosion to that of volumetric strain. In particular, the slope of the volumetric strain and eroded fraction curve ($d\varepsilon_v/df_{er}$) can be obtained from the DEM data in Fig. 4*(a)* for a range of samples. This data can then be plotted against the pre-shearing stress ratio, as shown in Fig. 6. The ratio ($d\varepsilon_v/df_{er}$) remains approximately constant when the stress ratio increases from 0 to close to 0.6. Within this range of the pre-shearing stress ratio, the confining stress appears to have less influence on the volumetric deformation of eroding sample. Beyond the pre-shearing stress ratio of approximately 0.6, a further increase in the pre-shearing stress ratio hinders the volumetric deformation, evidenced by the reduction of $d\varepsilon_v/df_{er}$. As the pre-shearing stress ratio surpasses its critical value of approximately 0.85, it is interesting to notice that $d\varepsilon_v/df_{er}$ changes its sign from positive to negative, suggesting that internal erosion at a high pre-shearing stress ratio in this type of DEM simulation would cause the soil sample to undergo dilation (i.e. $d\varepsilon_v < 0$).

The above observation of the rate of change of volumetric strain caused by internal erosion suggests that, at a small pre-shearing stress ratio, internal erosion would only cause the soil sample to purely undergo volumetric deformation. However, our simulations show that with higher pre-shearing stress ratios, internal erosion would cause the sample to undergo both volumetric and shear deformations, which will be discussed in the next section. The data presented in Fig. 6 can be best fit by the following equation:

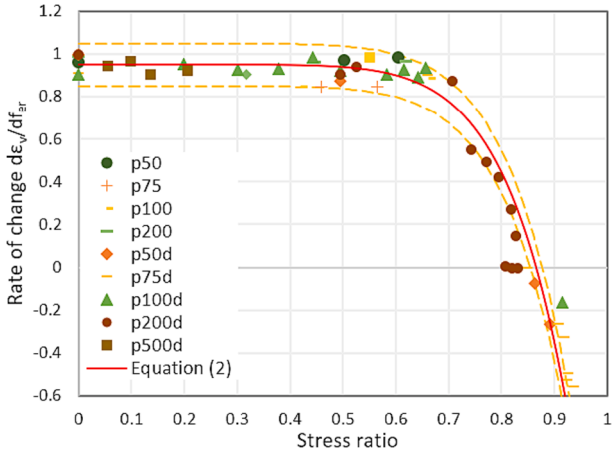

Fig. 6. Rate of change of volumetric strain with erosion at different stress ratios.

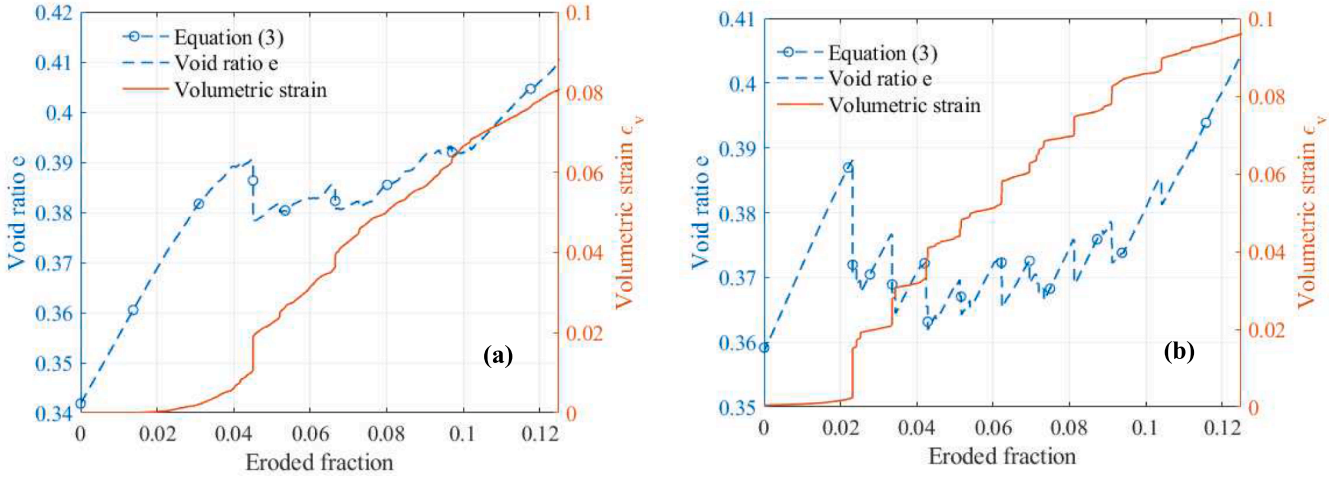

Fig. 5. Evolutions of volumetric strain and void ratio due to internal erosion of samples under confining stress of 100 kPa and pre-shearing stress ratio of η = 0 (a) and η = 0.55 (b).

$$\frac{d\varepsilon_v}{df_{er}} = A\left[1 - \left(\frac{\eta}{M_c}\right)^{\xi}\right] \tag{2}$$

where A and ξ are fitting parameters and M_c is the critical state stress ratio. For $A = 0.85$, $\xi = 8$ and $M_c = 0.86$, *Equation (2)* can best fit the DEM simulation data, as illustrated by the continuous red line in Fig. 6.

From the constitutive modelling point of view, *Equation (2)* provides a direct connection between the internal erosion rate (df_{er}) and the induced volumetric deformation caused by internal erosion. When $\eta < M_c$, the sample will undergo volumetric compaction under the action of internal erosion. In contrast, the sample will undergo dilation and possibly reach its ultimate critical stage under the action of internal erosion when $\eta \geq M_c$. As a result, *Equation (2)* enables the description of constitutive responses of soil specimens subjected to the combined loads (i.e. erosion and shearing). To this end, it is recommended to consider the volumetric strain as the primary indicator to account for the influence of internal erosion on the volumetric behaviour of eroded soil samples. The void ratio can then becomes a secondary parameter, which can be computed so long as the eroded fraction f_{er} and volumetric strain ε_v are known. For example, the change in the void ratio of a soil sample caused by internal erosion can be calculated as follows:

$$e = \frac{e_0 + f_{er}}{1 - f_{er}} - \varepsilon_v \frac{e_0 + 1}{1 - f_{er}} \tag{3}$$

where e_0 is the initial void ratio of the specimen, ε_v is the sample volumetric deformation and f_{er} is the eroded fraction.

3.3. Shearing behaviour of granular soils due to internal erosion

There has been a significant lack of investigations on the internal erosion-induced shearing behaviour of eroded soils. This is mainly because of the lack of standardised experimental apparatus capable of maintaining the shearing (or deviatoric) stress while causing internal erosion inside the soil specimen (Ke and Takahashi, 2012; Xiao and Shwiyhat, 2012; Li et al., 2020; Yang, 2019). However, it will be shown later in this study that soil samples are highly susceptible to shear failure when being eroded under high pre-shearing stress ratios. For instance, Fig. 7 illustrates the stress–strain (Fig. 7*a*) and volumetric (Fig. 7*b*) relationship of two p100d samples throughout the entire process outlined in Fig. 2, encompassing pre-shearing, erosion of up to 10 %, and post-erosion shearing behaviours. As observed in Fig. 7, the internal erosion process causes soil samples to undergo not only volumetric deformation but also shear deformation, with a higher pre-shearing stress ratio resulting in increased shear deformation, emphasizing the impracticality of neglecting the shearing-like behaviour caused by internal erosion. (Chang and Zhang, 2011). Therefore, in this study, the deviatoric strain of soil samples caused by internal erosion is recorded for different pre-shearing stress ratios and plotted against the volumetric strain, as shown in Fig. 8. In this figure, the slope of plotted lines represents the dilatancy behaviour of the soil samples caused by internal erosion. Since all deformations caused by internal erosion are unrecoverable, the dilatancy discussed in this paper can be represented by irrecoverable (plastic) deformation. Furthermore, to provide a reference view, the drained triaxial shearing behaviour of a non-eroded soil sample is also included in this figure, as illustrated by the yellow dash-line in Fig. 8. For each pre-shearing stress ratio, the blue dot marked on each plotted line represents the stage at which the internal erosion started to occur (also see points B and B' in Fig. 3*(b)*) and their location varies for different pre-shearing stress ratios. The drained triaxial shearing behaviour of the non-eroded soil sample exhibits an initial compaction response ($\delta\varepsilon_v > 0$), followed by dilation ($\delta\varepsilon_v < 0$) before reaching its critical state (i.e., refer to the yellow dash-line in Fig. 8). On the other hand, the shearing behaviour of the soil sample caused by internal erosion (i.e., pre-shearing stress was kept unchanged during the test) could be markedly different, depending on the initial pre-shearing

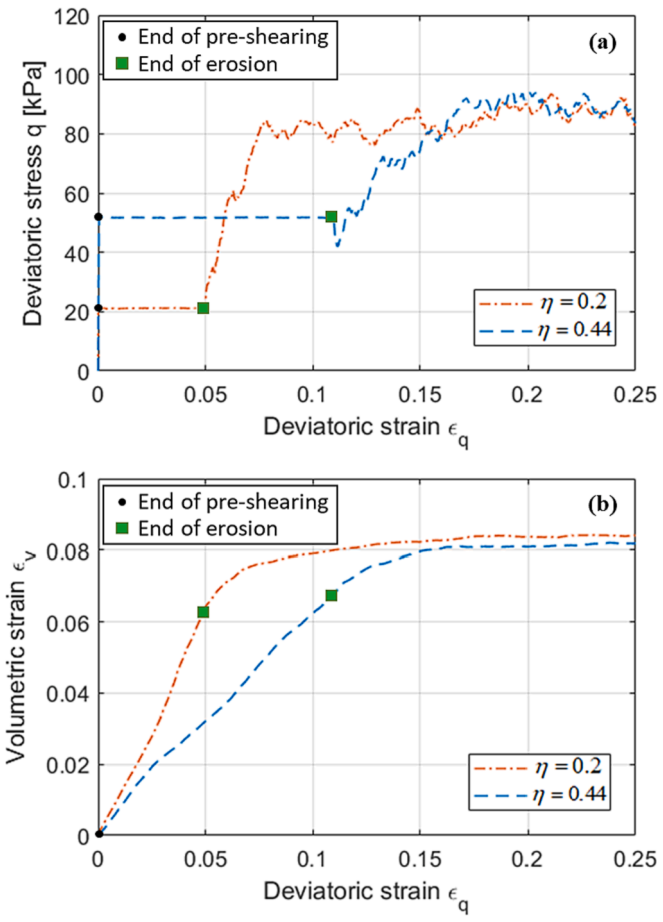

Fig. 7. Stress–strain (a) and volumetric (b) behaviours of DEM sample p100d underwent 10% erosion at two different pre-shearing stress ratios.

stress ratio or the behaviour of the sample before being subjected to the internal erosion process. Samples that carry a relatively small pre-shearing stress ratio (e.g., less than 0.66) and have already undergone initial compaction continue to undergo the compaction behaviour when subjected to the internal erosion process. The deviatoric strain continuously increases until the internal erosion stops. In contrast, in samples that carry a relatively large pre-shearing stress ratio (e.g., larger than 0.8 for both confining stresses in Fig. 8*(a)* and Fig. 8*(b)*) and have already undergone contraction and dilation, the internal erosion causes the sample to continue to dilate with increasing deviatoric strain. These observations suggest that a pre-shearing soil sample tends to maintain its pre-shearing behaviour when subjected to further internal erosion. However, in samples that have already undergone dilation, depending on the pre-shearing stress ratio, the internal erosion process would modify their behaviour from dilation to compaction, as in the case of $\eta = 0.87$ in Fig. 8*a* or $\eta = 0.8$ in Fig. 8*b* for different confining stresses. In some cases, when the pre-shearing stress ratio is high, the soil sample becomes extremely susceptible to internal erosion. For example, at the high pre-shearing stress ratio of $\eta = 0.93$ in Fig. 8*(a)* or $\eta = 0.91$ in Fig. 8 *(b)*, a small eroded fraction (0.9 % for $\eta = 0.93$ and 1.38 % for $\eta = 0.91$) causes the soil sample to dilate and reach its critical state continuously.

The above observation on the behaviour of a soil sample subjected to a high pre-shearing stress ratio and subsequent internal erosion can be explained in a similar way to that caused by an external loading process (or drained triaxial shearing without erosion). For instance, under the action of continuous external loads, the number of soil particles remains unchanged in the soil sample. As a result, the increase in applied external load causes changes to stresses acting on soil particles through the force chain network within the granular system, facilitating the

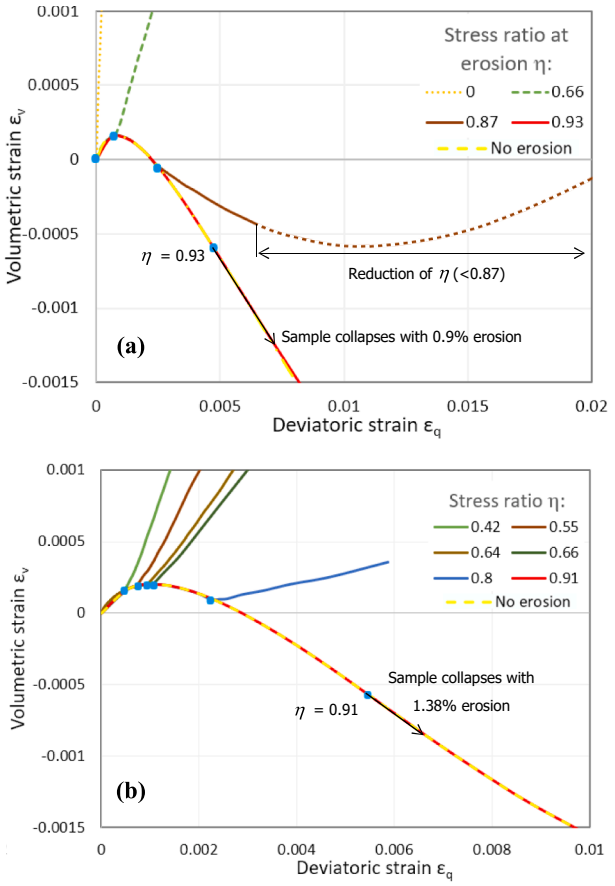

Fig. 8. Volumetric behaviour while erosion: a. p75d samples and b. p100d samples.

shearing deformation. On the other hand, in internal erosion, the applied external loads usually remain constant, whilst the number of particles in the system continuously reduces, leading to the redistribution of stresses acting on soil particles remaining in the granular system. The redistribution of stresses in the granular system caused by internal erosion usually leads to an increase in the average stress of the major force chain, which replicates the action of the continuous externally applied loads on the soil sample. This explains why the shearing behaviour of samples under a high pre-shearing stress ratio caused by internal erosion follows the same behaviour of non-eroded samples undergoing continuous shearing. On the other hand, at lower pre-shearing stresses (e.g., smaller than 0.9), internal erosion modifies the shearing behaviour of soil samples. It is commonly accepted that internal erosion causes the soil sample to undergo volumetric compaction, and this is true for the case of no or low pre-shearing stress ratios. However, under a relatively high pre-shearing stress, where the soil sample has started undergoing dilation, internal erosion causes competition between compaction (due to the fixed external applied load and mass loss) and dilation (due to pre-shearing dilation) shearing behaviours of the soil sample. The dominant response of the soil sample caused by internal erosion depends on the amount of dilation the soil sample experiences before the internal erosion starts. Specifically, for a soil sample undergoing dilation shearing before being subjected to internal erosion, losing grains would cause the sample to become looser, preventing particles from sliding over each other (i.e., dilation). At the same time, losing grains would cause an increase in the stress carried by soil particles, encouraging the dilative response of the soil specimen in a similar way to that caused by applying mechanical loads.

Fig. 9 shows the evolution of dilatancy ($d\varepsilon_v^p/d\varepsilon_s^p$) caused by internal erosion for different pre-shearing stress ratios. For each pre-shearing

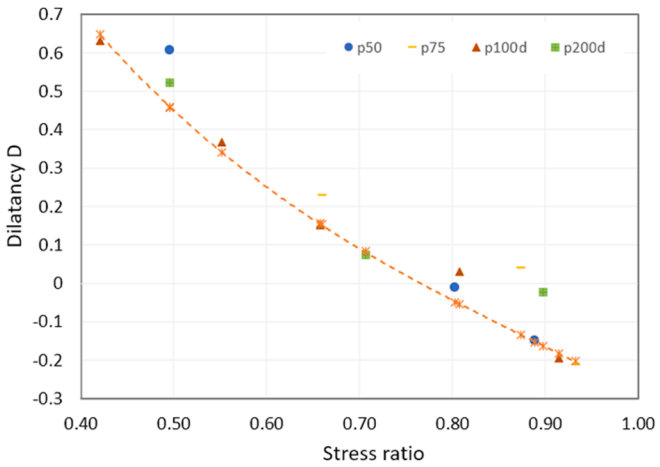

Fig. 9. Evolution of dilatancy caused by internal erosion for different pre-shearing stress ratios.

stress ratio, the dilatancy response of the soil sample caused by internal erosion is represented by a single dot point in Fig. 9. This is because the dilatancy caused by internal erosion remains more and less unchanged, as shown in Fig. 8, where the volumetric strain exhibits an almost linear development with increasing shear strain until the sample can no longer maintain a constant pre-shearing stress ratio (i.e., collapse). Consequently, the dilatancy caused by internal erosion for each simulation can be approximated as the slope of a linear trendline representing the relatively linear section of the volumetric strain and shear strain curve.

To describe the dependence of dilatancy on pre-shearing stress ratio caused by internal erosion under different pre-shearing stress ratios, a statistical equation can be drawn from this DEM data. This equation takes the following parabolic form:

$$D = \frac{d\varepsilon_v^p}{d\varepsilon_s^p} = \frac{M_c^2 - \eta^2}{\beta\eta} \tag{4}$$

where M_c is a constant parameter and can be taken as the critical state friction coefficient or critical state stress ratio; η is the pre-shearing stress ratio; and β is a fitting parameter. For the DEM data presented in Fig. 9, the best-fit result (i.e. orange dash-line) suggested $\beta = 1.5$. It is noted that *Equation (4)* shares a similar form to the original dilatancy model of the modified Cam-clay constitutive model, for which $\beta = 2$. This undoubtedly supports earlier explanation that mass extraction due to internal erosion results in similar dilatancy behaviour found in the volumetric hardening framework. It is also worth noting that *Equation (4)* reflects well the volumetric behaviour of soil samples subjected to internal erosion at zero stress ratio $\eta = 0$, as shown in Fig. 8*(a)*. This is not possible for several existing dilatancy models, including the popular one of the deviatoric hardening framework, which takes the following form: $D = A_d(M_d - \eta)$ (Dafalias and Manzari, 2004), where A_d is a constant related to the material fabric and M_d is the stress ratio at zero dilatancy. This suggests that if one would like to adopt the deviatoric constitutive modelling framework to describe the behaviour of granular materials undergoing internal erosion, two different dilatancy models would be required, one for external loading and the other for internal erosion.

4. Conclusions

The effect of internal erosion on the mechanical behaviour of gap-graded cohesionless soils was investigated in this study by carrying out a series of DEM simulations. Particular attention was placed on the influence of the pre-shearing stress ratios on the mechanical responses of samples undergoing internal erosion, a factor that existing experimental

setups are unable to replicate. Based on the simulation results, the following conclusions can be made:

a. When a soil sample is subjected to internal erosion, deformation only occurs after a certain amount of erosion, called the suffosion point. This point represents the amount of loosely/non-loaded particles in the soil specimen, which varies depending on the mobilised shear strength of the soil sample represented by a pre-shearing stress ratio. The higher the pre-shearing stress ratio, the lower the suffosion point. A new concept of suffosion surface was proposed to provide a criterion for deciding when the deformation (i.e., suffosion) would occur in the constitutive description of eroded soils.
b. After the suffosion point, the soil sample undergoes both volumetric and shearing responses. Granular assemblies tend to remain in their state prior to erosion. If they are under compaction, they will continue to be compacted. In contrast, if they are dilating, they will continue to dilate.
c. The volumetric strain is found to be a better primary indicator to indicate the deformation caused by internal erosion compared to the commonly used void ratio, which has a limited capacity to describe internal erosion after a certain amount of mass loss. A new statistical equation was proposed to provide a link between the rate change of volumetric strain and that of internal erosion.
d. The dilatancy behaviour of granular assemblies caused by internal erosions appears to differ from that caused by shearing loads. This suggests that if one wants to adopt a deviatoric hardening constitutive modelling framework to describe the behaviour of eroded soils, an additional dilatancy rule is required to describe the volumetric behaviour of the materials due to internal erosion.

Finally, it is also worth mentioning that this study has several limitations that can be further improved in future works. The coarse and fine particles in this study are all spherical and have the same properties. In reality, a mixing of different types of soil grains would more likely be the case. Thus, it is suggested to use different friction and rolling friction angles in future studies.

CRediT authorship contribution statement

Tien V. Nguyen: Formal analysis, Investigation, Methodology, Software, Validation, Visualization, Writing – original draft. **Ha H. Bui:** Conceptualization, Funding acquisition, Investigation, Methodology, Project administration, Resources, Supervision, Writing – review & editing. **Khoa M. Tran:** Investigation, Writing – review & editing. **Giang D. Nguyen:** Conceptualization, Funding acquisition, Investigation, Methodology, Writing – review & editing. **Asadul Haque:** Investigation, Writing – review & editing.

Declaration of competing interest

The authors declare that they have no known competing financial interests or personal relationships that could have appeared to influence the work reported in this paper.

Data availability

Data will be made available on request.

Acknowledgement

The authors gratefully acknowledge the financial support from the Australian Research Council via Discovery Projects DP190102779 (Bui & Nguyen) and FT200100884 (Bui). Part of this research was undertaken with the assistance of resources and services from the National Computational Infrastructure (NCI), supported by the Australian Government.

References

Burenkova, V., 1993. *Assessment of suffusion in non-cohesive and graded soils.* Filters in geotechnical and hydraulic engineering. Balkema, Rotterdam 357–360.
Cavarretta, I., Coop, M., C. o'sullivan,, 2010. The influence of particle characteristics on the behaviour of coarse grained soils. Géotechnique 60 (6), 413–423.
Chang, D., Zhang, L., 2011. A Stress-controlled Erosion Apparatus for Studying Internal Erosion in Soils. Geotech. Test. J. 34 (6), 579–589.
Chang, D.S., Zhang, L.M., 2013. Critical Hydraulic Gradients of Internal Erosion under Complex Stress States. J. Geotech. Geoenviron. Eng. 139 (9), 1454–1467.
Chang, D.S., Zhang, L.M., 2013. Extended internal stability criteria for soils under seepage. Soils Found. 53 (4), 569–583.
Cundall, P.A., Strack, O.D., 1979. A discrete numerical model for granular assemblies. Geotechnique 29 (1), 47–65.
Dafalias, Y.F., Manzari, M.T., 2004. Simple plasticity sand model accounting for fabric change effects. J. Eng. Mech. 130 (6), 622–634.
Dai, B.B., Yang, J., Zhou, C.Y., 2016. Observed effects of interparticle friction and particle size on shear behavior of granular materials. Int. J. Geomech. 16 (1), 04015011.
Fannin, J., 2008. Karl Terzaghi: From theory to practice in geotechnical filter design. J. Geotech. Geoenviron. Eng. 134 (3), 267–276.
Fisher, W.D., Camp, T.K., Krzhizhanovskaya, V.V., 2016. Crack detection in earth dam and levee passive seismic data using support vector machines. Procedia Computer Science 80, 577–586.
Hicher, P.-Y.-J.-G., 2013. Modelling the impact of particle removal on granular material behaviour. Geotechnique 63 (2), 118–128.
Hieu, D.M., Kawamura, S., Matsumura, S., 2017. Internal erosion of volcanic coarse grained soils and its evaluation. International Journal of Geomate 13 (38), 165–172.
Hosn, R.A., et al., 2018. A discrete numerical model involving partial fluid-solid coupling to describe suffusion effects in soils. Comput. Geotech. 95, 30–39.
Hu, Z., Zhang, Y., Yang, Z., 2019. Suffusion-induced deformation and microstructural change of granular soils: a coupled CFD–DEM study. Acta Geotech. 14 (3), 795–814.
Israr, J., Indraratna, B., Rujikiatkamjorn, C., 2016. Laboratory investigation of the seepage induced response of granular soils under static and cyclic loading. Geotech. Test. J. 39 (5), 795–812.
Jiang, X., et al., 2023. Internal erosion of debris-flow deposits triggered by seepage. Eng. Geol. 314, 107015.
Kawano, K., *Numerical Evaluation of Internal Erosion due to Seepage Flow*. Imperial College London, 2016.
Ke, L., Takahashi, A., 2012. Strength reduction of cohesionless soil due to internal erosion induced by one-dimensional upward seepage flow. Soils Found. 52 (4), 698–711.
Ke, L., Takahashi, A., 2014. Experimental investigations on suffusion characteristics and its mechanical consequences on saturated cohesionless soil. Soils Found. 54 (4), 713–730.
Ke, L., Takahashi, A., 2014. Triaxial erosion test for evaluation of mechanical consequences of internal erosion. Geotech. Test. J. 37 (2), 347–364.
Ke, L., Takahashi, A.J.S., Foundations, 2012. Strength reduction of cohesionless soil due to internal erosion induced by one-dimensional upward seepage flow. 52 (4), 698–711.
Kenney, T.C., Lau, D., 1985. INTERNAL STABILITY OF GRANULAR FILTERS. Can. Geotech. J. 22 (2), 215–225.
Kenney, T., Lau, D., 1986. Internal stability of granular filters: Reply. Can. Geotech. J. 23 (3), 420–423.
KÉZDI, Á., *Soil Physics: Selected Topics*. 1979, Amsterdam: Elsevier.
Kozicki, J., Donze, F.V., 2009. YADE-OPEN DEM: An open-source software using a discrete element method to simulate granular material. Eng. Comput.
Lafleur, J., Mlynarek, J., Rollin, A.L., 1989. Filtration of Broadly Graded Cohesionless Soils. J. Geotech. Eng. 115 (12), 1747–1768.
Lee, J.-S., Tran, M.K., Lee, C., 2012. Evolution of layered physical properties in soluble mixture: Experimental and numerical approaches. Eng. Geol. 143–144, 37–42.
Li, S., Russell, A.R., Muir Wood, D., 2020. Influence of particle-size distribution homogeneity on shearing of soils subjected to internal erosion. Can. Geotech. J. 57 (11), 1684–1694.
Mitchell, W., Fitzpatrick, M., 1979. An incident at Rowallan dam. in *Thirteenth International Congress on Large Dams*.
Mu, L., et al., 2023. Coupled CFD–DEM Investigation of Erosion Accompanied by Clogging Mechanism under Different Hydraulic Gradients. Comput. Geotech. 153, 105058.
Nguyen, C.D., et al., 2019. Experimental investigation of microstructural changes in soils eroded by suffusion using X-ray tomography. Acta Geotech. 14 (3), 749–765.
Nguyen, T.T., Indraratna, B., 2020. The energy transformation of internal erosion based on fluid-particle coupling. Comput. Geotech. 121, 103475.
Prasomsri, J., Shire, T., Takahashi, A., 2021. Effect of fines content on onset of internal instability and suffusion of sand mixtures. Géotechnique Letters 11 (3), 209–214.
Reclamation, B.o. *Teton Dam History*. 2016; Available from: https://www.usbr.gov/pn/snakeriver/dams/uppersnake/teton/index.html.
Sawicki, A. and W. Swidzinski. *Possible scenario of slope failure in Dychow water power plant*. in *Proc. XII Soil Mech. Foundation Eng. Conf.* 2000.
Scholtes, L., Hicher, P.-Y., Sibille, L., 2010. Multiscale approaches to describe mechanical responses induced by particle removal in granular materials Etude par approches multi-echelles de la reponse mecanique d'un milieu granulaire induite par l'extraction de ses particules. Comptes Rendus - Mecanique 338 (10–11), 627–638.
Sherard, J.L., 1992. 1992.. Sinkholes in dams of coarse, broadly graded soils. Conference on Embankment Dams. Publ by ASCE, Berkely, CA, USA.

Shire, T., et al., Fabric and Effective Stress Distribution in Internally Unstable Soils. Journal of Geotechnical and Geoenvironmental Engineering, 2014. **140**(12): p. 04014072 (11 pp.).
Slangen, P., Fannin, R., 2017. The role of particle type on suffusion and suffosion. Géotechnique Letters 7 (1), 6–10.
Strahler, A.W., Stuedlein, A.W., Arduino, P., 2018. Three-dimensional stress-strain response and stress-dilatancy of well-graded gravel. Int. J. Geomech. 18 (4), 04018014.
Tao, H., Tao, J., 2017. Quantitative analysis of piping erosion micro-mechanisms with coupled CFD and DEM method. Acta Geotech. 12 (3), 573–592.
Tran, K.M., et al., 2020. A DEM approach to study desiccation processes in slurry soils. Comput. Geotech. 120, 103448.
Tran, K.M., Bui, H.H., Nguyen, G.D., 2021. DEM modelling of unsaturated seepage flows through porous media. Computational Particle Mechanics.
Wan, C.F., Fell, R., 2008. Assessing the potential of internal instability and suffusion in embankment dams and their foundations. J. Geotech. Geoenviron. Eng. 134 (3), 401–407.
Wang, X., Li, J.J.A.M.S., 2015. On the degradation of granular materials due to internal erosion. 31 (5), 685–697.
Wang, X., Li, J., 2015. On the degradation of granular materials due to internal erosion. Acta Mech. Sin. 31 (5), 685–697.
Wei, L., Yang, J., 2014. On the role of grain shape in static liquefaction of sand–fines mixtures. Géotechnique 64 (9), 740–745.
Wood, D.M., Maeda, K., Nukudani, E., 2010. Modelling mechanical consequences of erosion. Geotechnique 60 (6), 447–457.
Xiao, Y., et al., 2017. Model predictions for behaviors of sand-nonplastic-fines mixturesusing equivalent-skeleton void-ratio state index. Sci. China Technol. Sci. 60 (6), 878–892.
Xiao, Y., et al., 2017. Strength–dilatancy relation of sand containing non-plastic fines. Géotechnique Letters 7 (2), 204–210.
Xiao, M., Shwiyhat, N.J.G.T.J., 2012. Experimental investigation of the effects of suffusion on physical and geomechanic characteristics of sandy soils. 35 (6), 890–900.
Xiao, M., Shwiyhat, N., 2012. Experimental investigation of the effects of suffusion on physical and geomechanic characteristics of sandy soils. Geotech. Test. J. 35 (6), 890–900.
Xu, M., Song, E., Chen, J., 2012. A large triaxial investigation of the stress-path-dependent behavior of compacted rockfill. Acta Geotech. 7 (3), 167–175.
Yang, J., et al., 2019. Analysis of suffusion in cohesionless soils with randomly distributed porosity and fines content. Comput. Geotech. 111, 157–171.
Ye, Z., Liu, H., 2021. Investigating the relationship between erosion-induced structural damage and lining displacement parameters in shield tunnelling. Comput. Geotech. 133, 104041.
Zhang, F., et al., 2019. Three-dimensional DEM modeling of the stress–strain behavior for the gap-graded soils subjected to internal erosion. Acta Geotech. 14 (2), 487–503.
Zhou, W., et al., 2016. DEM analysis of the size effects on the behavior of crushable granular materials. Granul. Matter 18 (3), 1–11.